Turbulence spectra from a tidal channel

By H. L. GRANT, R. W. STEWART† AND A. MOILLIET

Pacific Naval Laboratory of the Defence Research Board of Canada,
Esquimalt, B.C., Canada

J. Fluid Mechanics, 1962

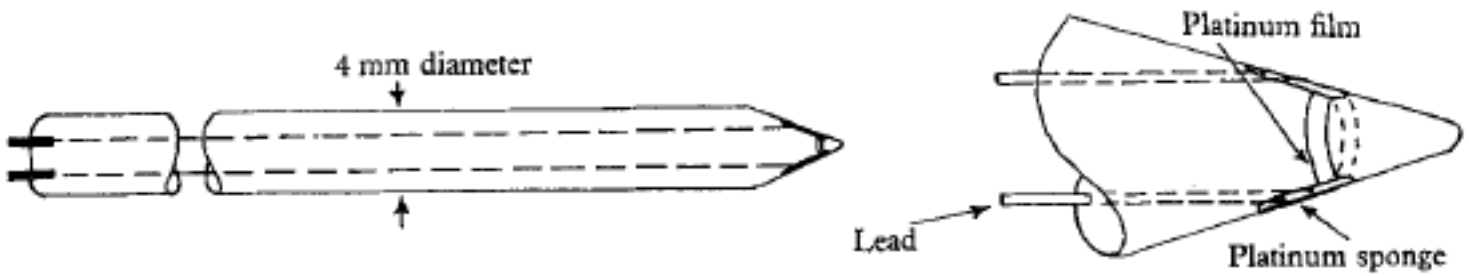

FIGURE 1. The hot-film probe.

Grant etal 1962

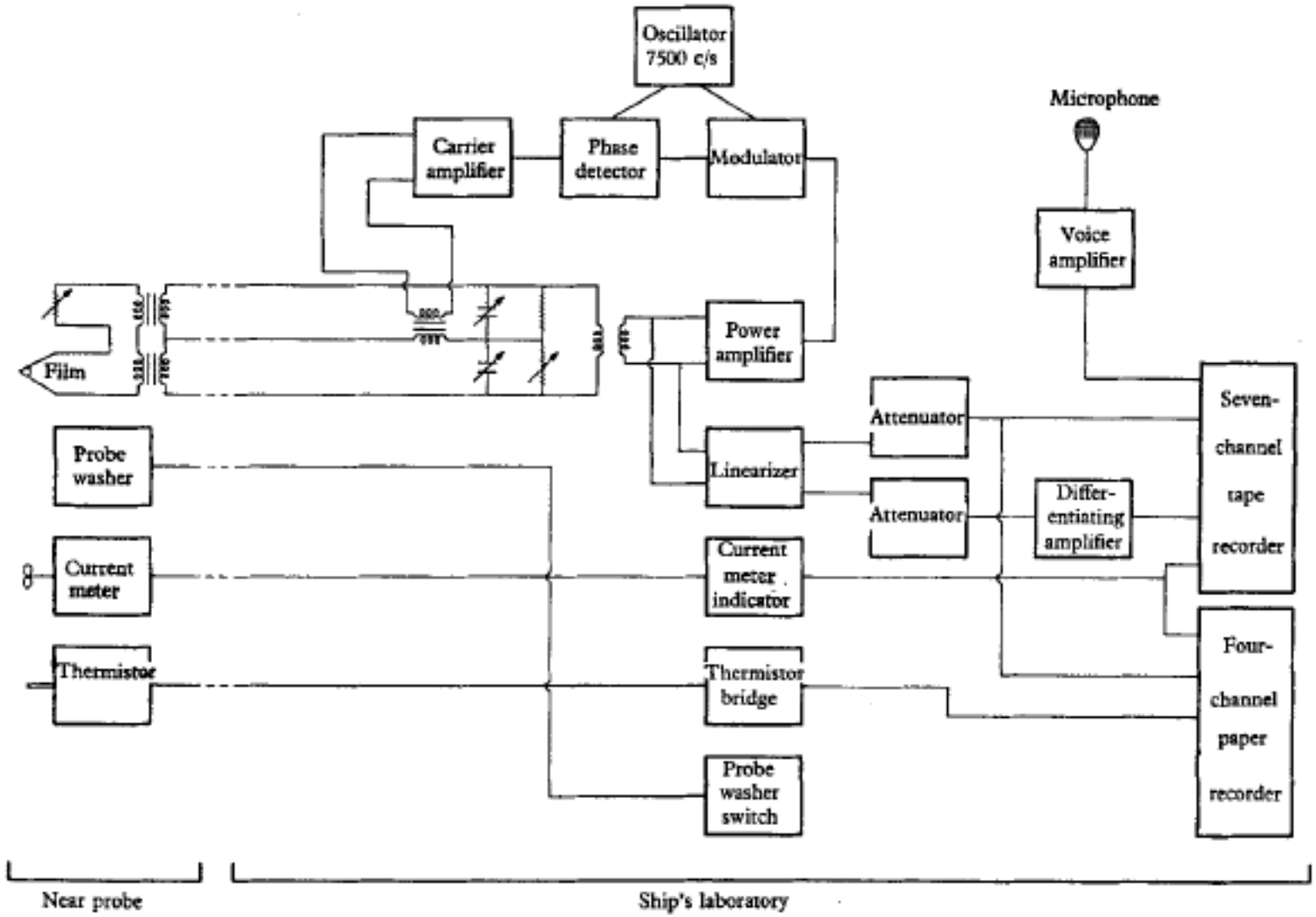

FIGURE 2. Simplified block diagram of the hot film flow-meter and recording equipment.

Grant etal 1962

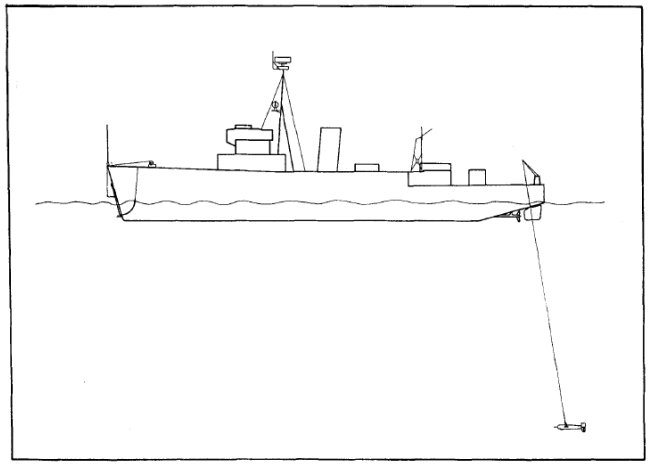

FIGURE 3. The research vessel *Oshawa*, showing the probe mounts on the bow and on the towed body. The overall length of the ship is 217 ft.

FIGURE 5. The nose of the towed body.

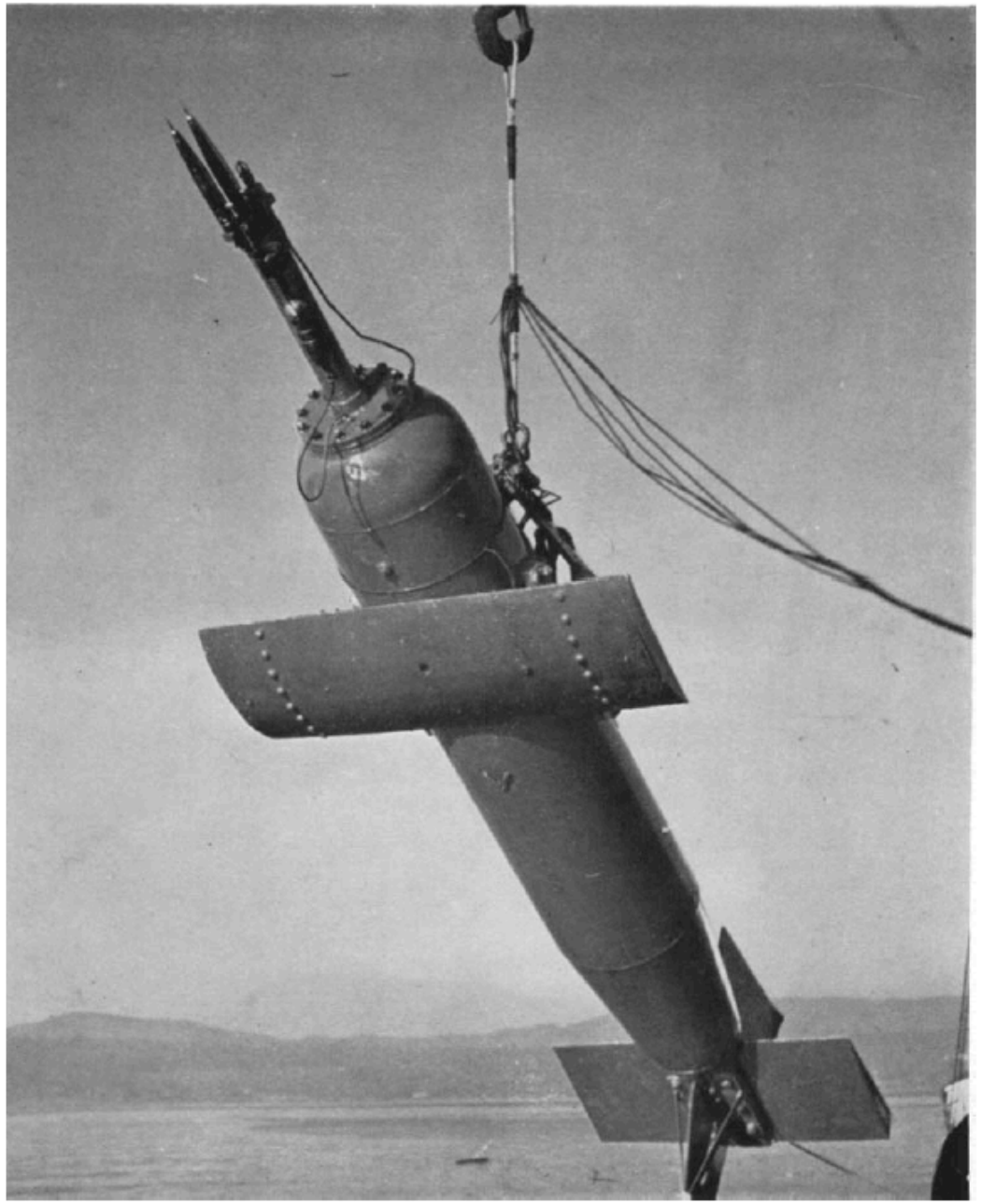

FIGURE 4. The towed body.

Grant etal 1962

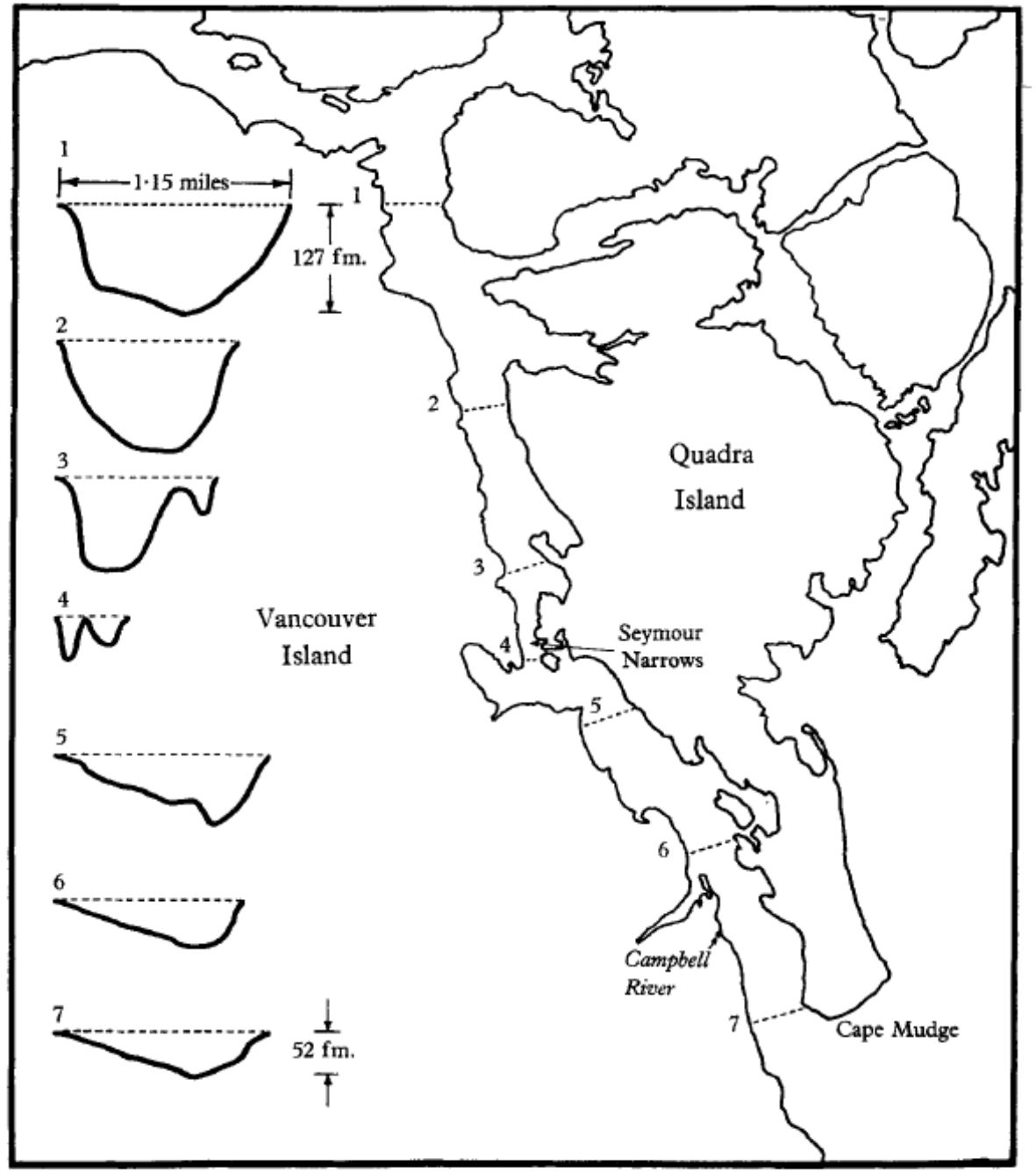

FIGURE 6. Plan of Discovery Passage. (For more detail, refer to the chart listed in the references.)

Grant etal 1962

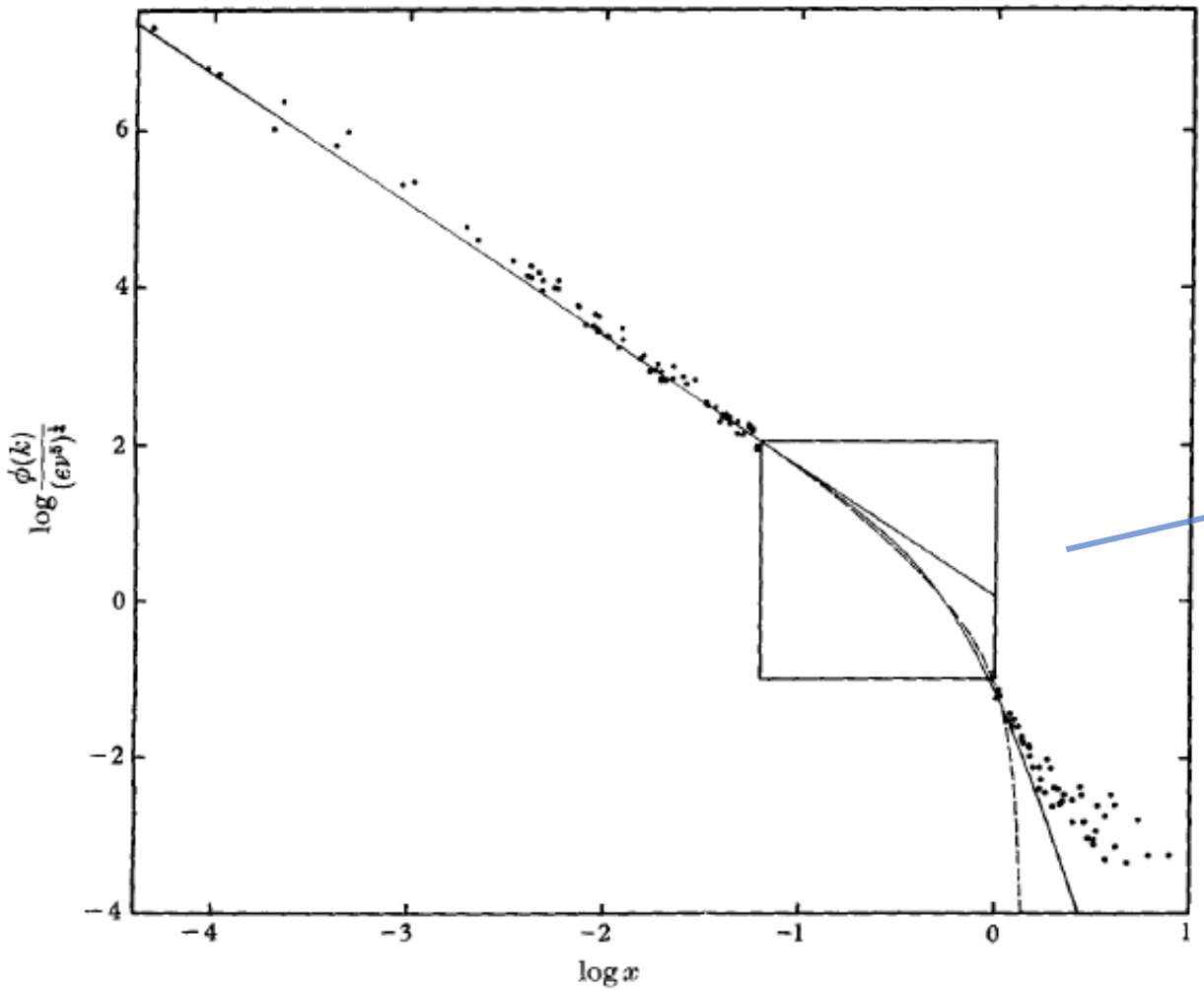

FIGURE 12. Seventeen spectra compared to the theories of Kolmogoroff, Heisenberg and Kovasznay. The straight line has a slope of $-\frac{5}{3}$, the curved solid line is Heisenberg's theory and the dashed line is Kovasznay's theory. Within the square, the observations are too crowded to display on this scale and they are shown in figure 13.

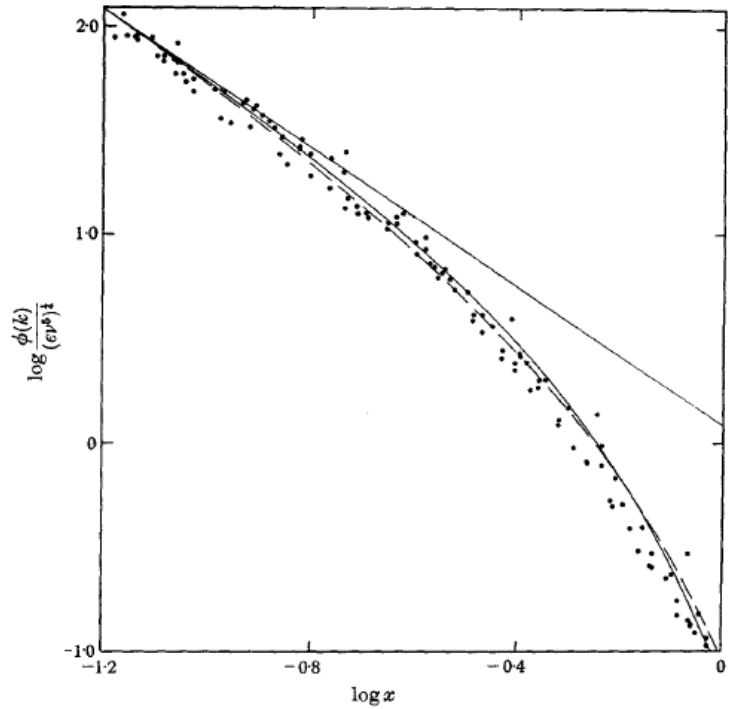

FIGURE 13. The collected spectra in the low wave-number end of the dissipation range.

Grant etal 1962

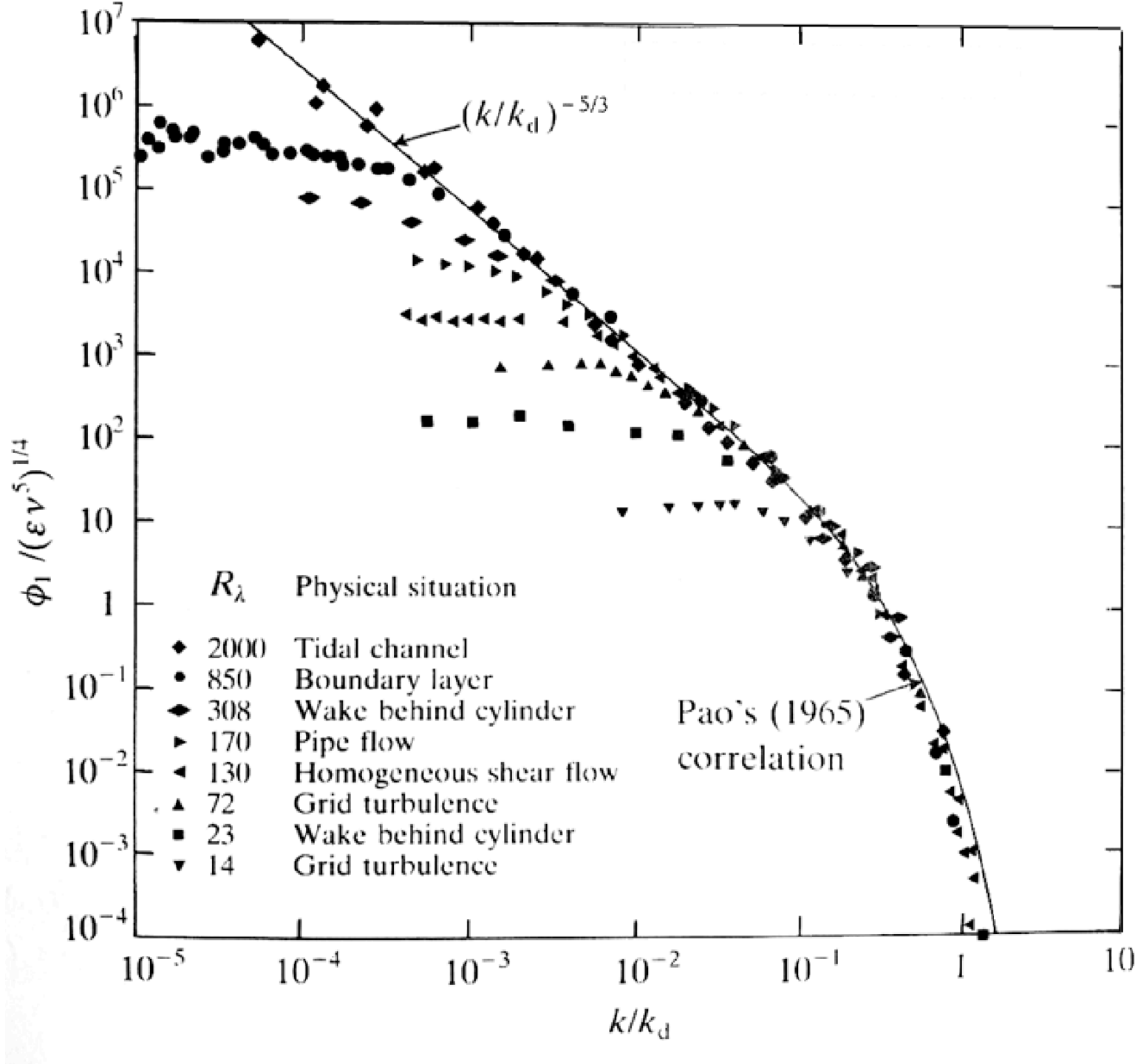

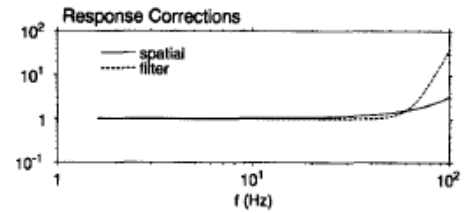
Response Corrections
spatial
filter
f (Hz)

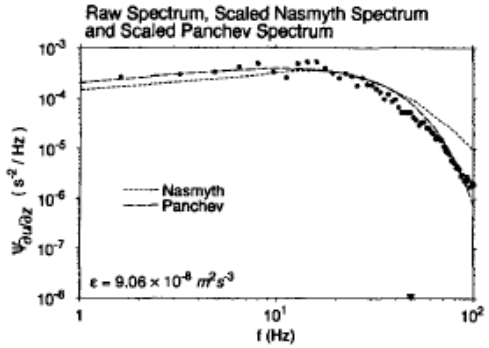
Raw Spectrum, Scaled Nasmyth Spectrum
and Scaled Panchev Spectrum
Nasmyth
Panchev
ε = 9.06 × 10⁻⁸ m²s⁻³
f (Hz)

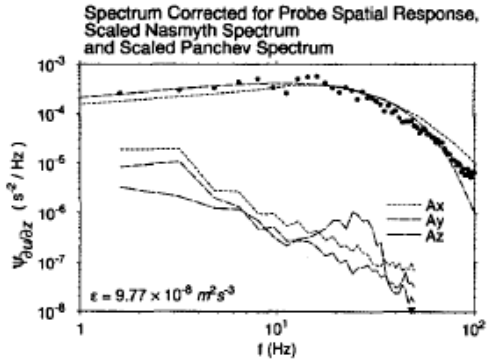
Spectrum Corrected for Probe Spatial Response,
Scaled Nasmyth Spectrum
and Scaled Panchev Spectrum
Ax
Ay
Az
ε = 9.77 × 10⁻⁸ m²s⁻³
f (Hz)

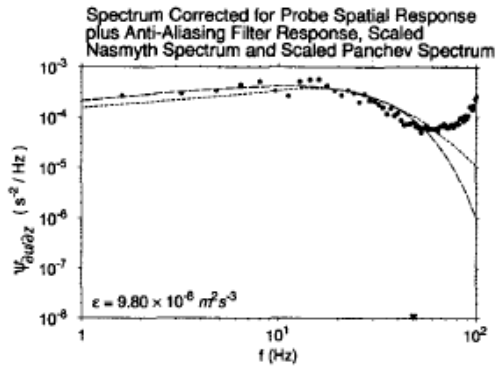
Spectrum Corrected for Probe Spatial Response
plus Anti-Aliasing Filter Response, Scaled
Nasmyth Spectrum and Scaled Panchev Spectrum
ε = 9.80 × 10⁻⁶ m²s⁻³
f (Hz)

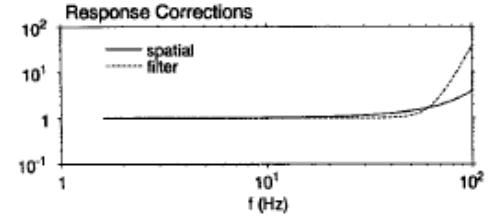
Response Corrections
spatial
filter
f (Hz)

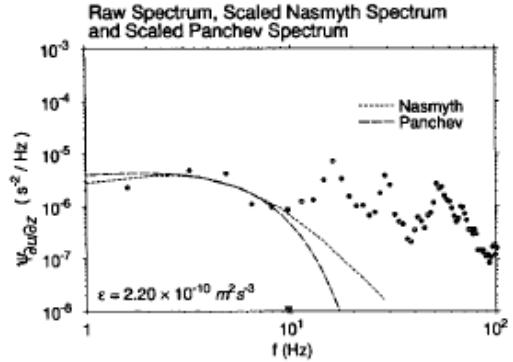
Raw Spectrum, Scaled Nasmyth Spectrum
and Scaled Panchev Spectrum
Nasmyth
Panchev
ε = 2.20 × 10⁻¹⁰ m²s⁻³
f (Hz)

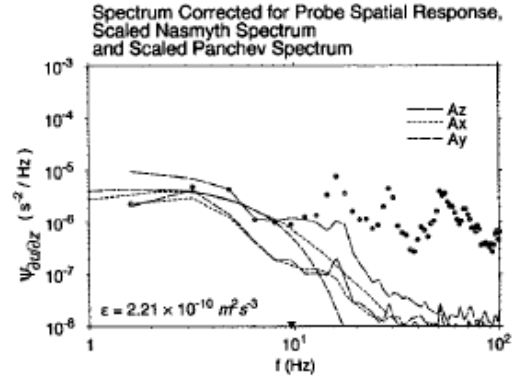
Spectrum Corrected for Probe Spatial Response,
Scaled Nasmyth Spectrum
and Scaled Panchev Spectrum
Az
Ax
Ay
ε = 2.21 × 10⁻¹⁰ m²s⁻³
f (Hz)

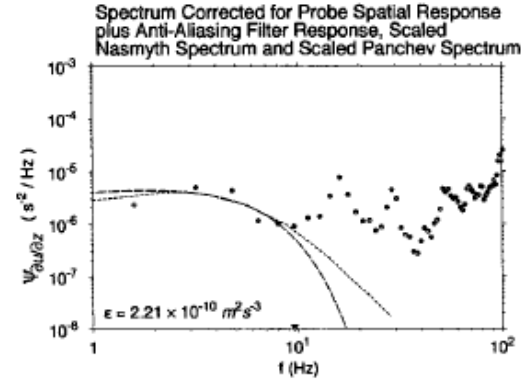
Spectrum Corrected for Probe Spatial Response
plus Anti-Aliasing Filter Response, Scaled
Nasmyth Spectrum and Scaled Panchev Spectrum
ε = 2.21 × 10⁻¹⁰ m²s⁻³
f (Hz)

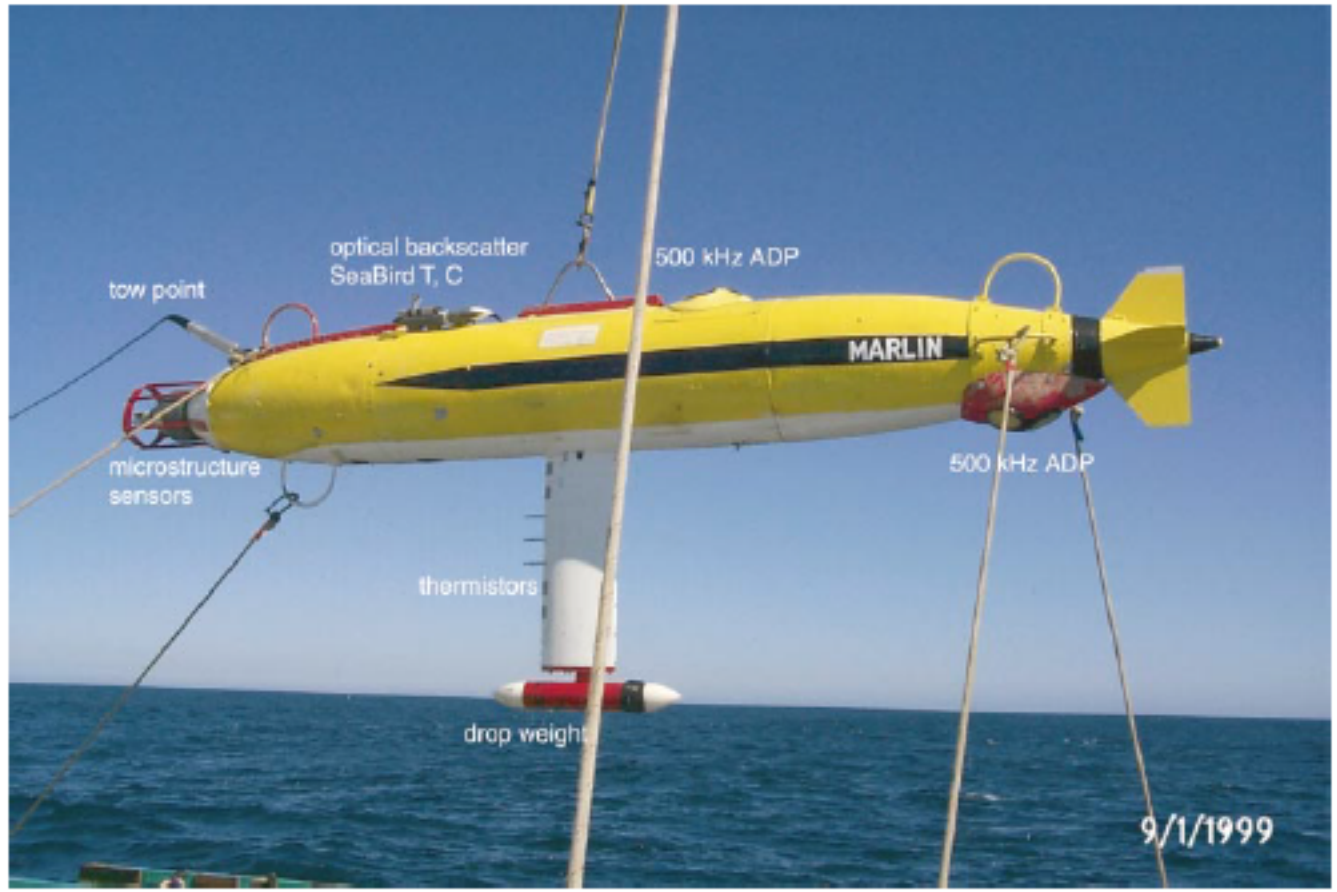

FIG. 1. MARLIN suspended from the ship's crane over the side of R/V *Wecoma*. Four tag lines are attached to body hoops and another (foreground) to the crane's headache ball. Locations of sensors discussed in the text are indicated. The obstacle avoidance sonar is flush with the hull.

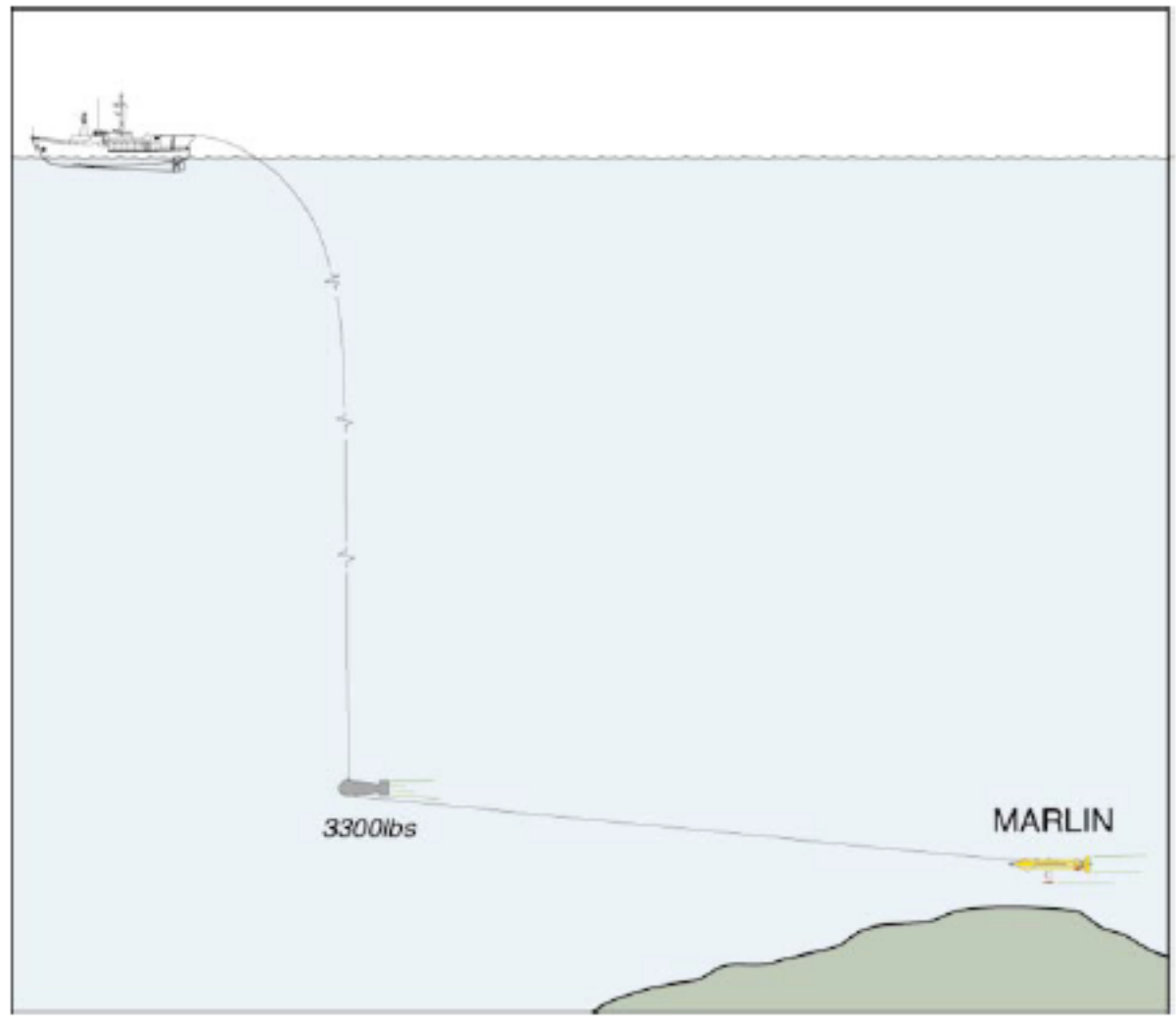
3300lbs
MARLIN

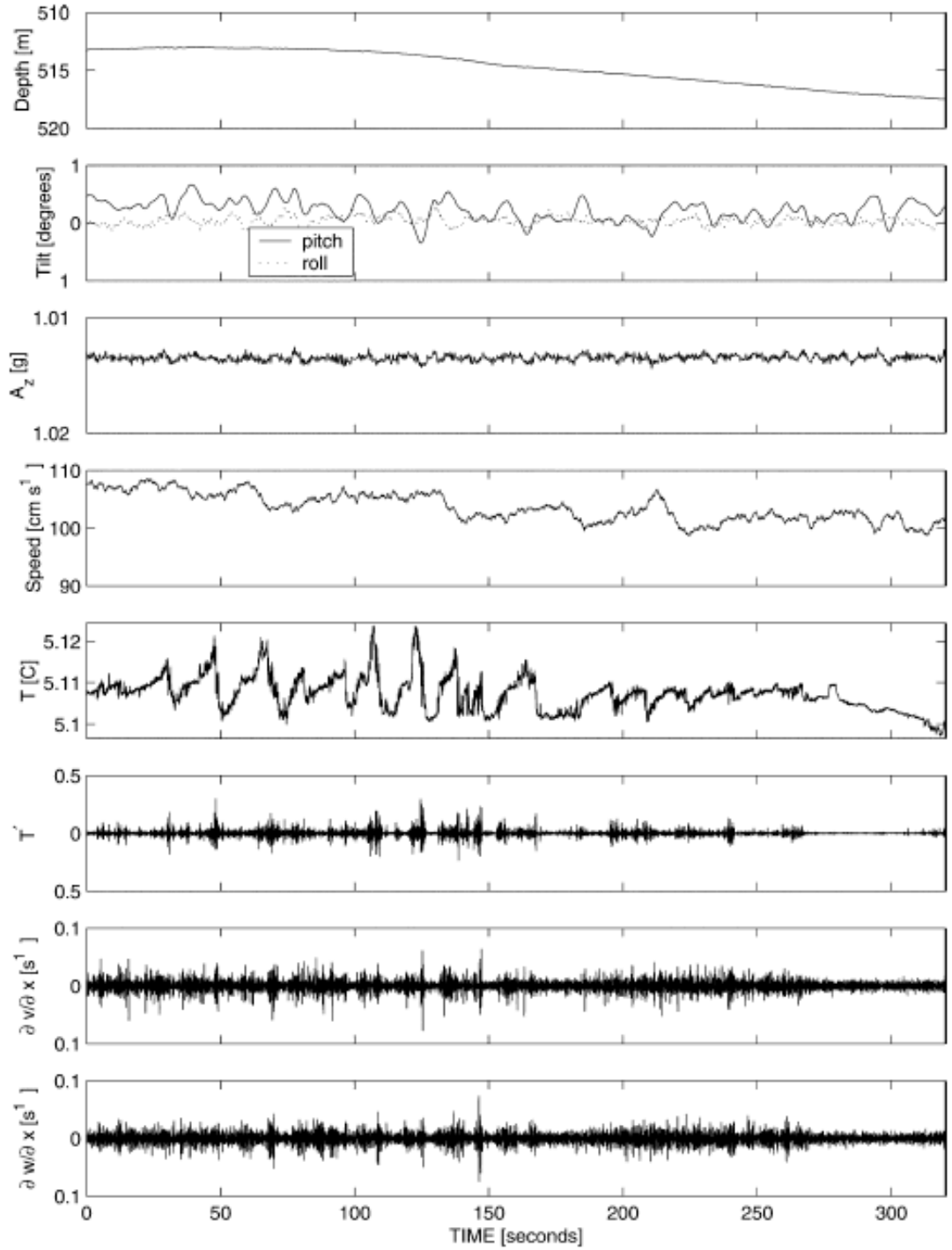
Depth [m]
510
515
520
Tilt [degrees]
1
0
1
pitch
roll
A_z [g]
1.01
1.02
Speed [cm s^-1]
110
100
90
T [C]
5.12
5.11
5.1
T'
0.5
0
0.5
∂ w/∂ x [s^-1]
0.1
0
0.1
∂ w/∂ x [s^-1]
0.1
0
0.1
0
50
100
150
200
250
300
TIME [seconds]

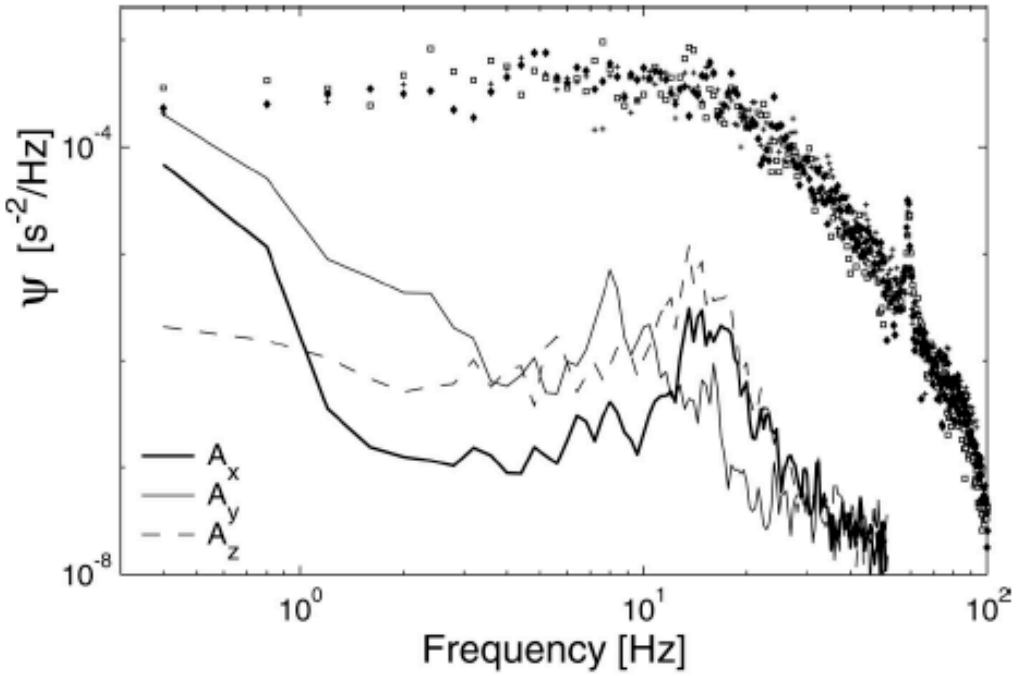
ψ [s-2/Hz]
10-4
10-8
A x
A y
A z
100
101
102
Frequency [Hz]

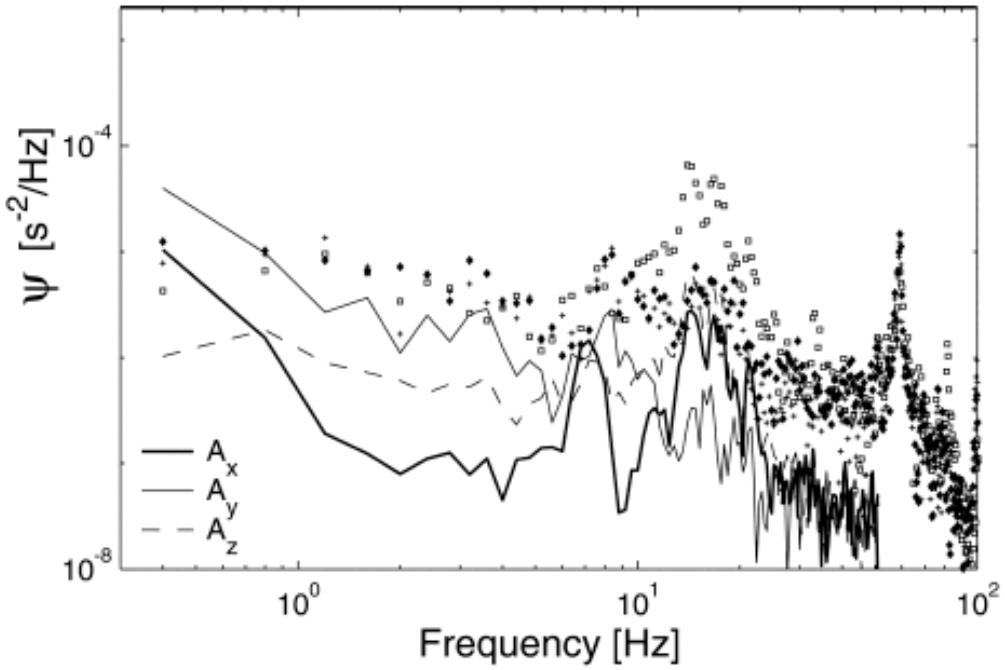
ψ [s-2/Hz]
10-4
10-8
A x
A y
A z
100
101
102
Frequency [Hz]

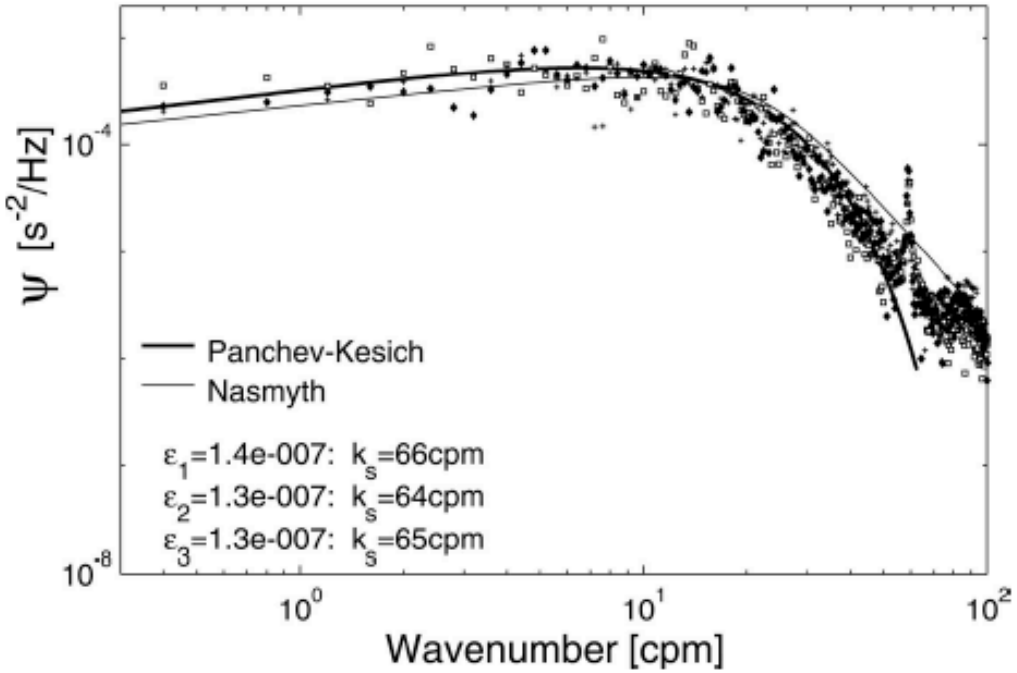
ψ [s-2/Hz]
10-4
10-8
Panchev-Kesich
Nasmyth
ε1=1.4e-007: ks=66cpm
ε2=1.3e-007: ks=64cpm
ε3=1.3e-007: ks=65cpm
100
101
102
Wavenumber [cpm]

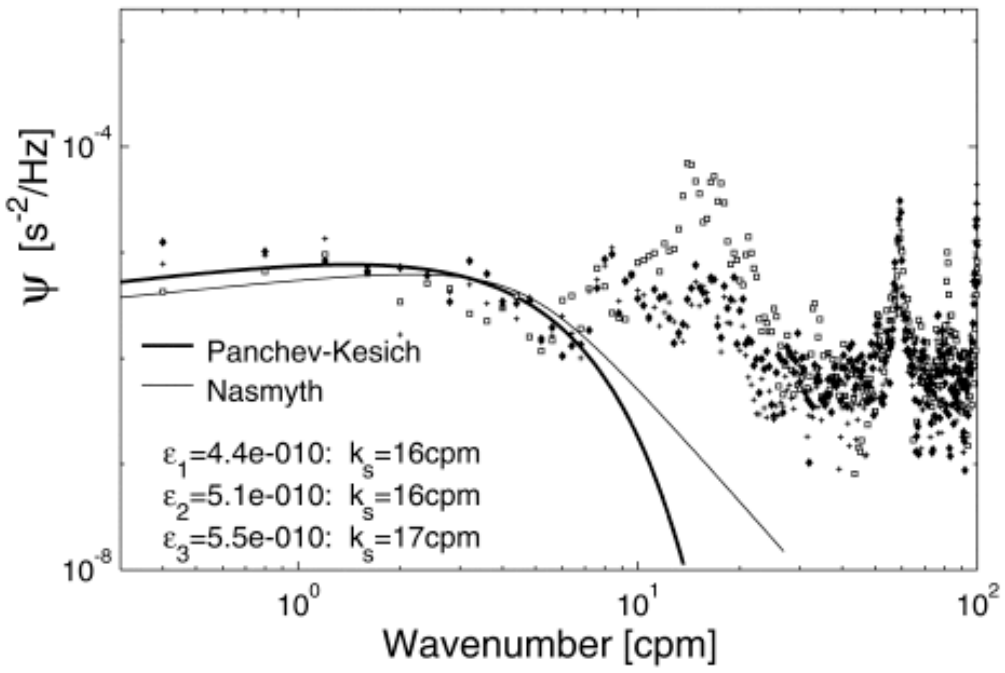
ψ [s-2/Hz]
10-4
10-8
Panchev-Kesich
Nasmyth
ε1=4.4e-010: ks=16cpm
ε2=5.1e-010: ks=16cpm
ε3=5.5e-010: ks=17cpm
100
101
102
Wavenumber [cpm]

Gargett etal 1984

J. Fluid Mech. (1984), *vol.* 144, *pp.* 231–280
Printed in Great Britain

Local isotropy and the decay of turbulence in a stratified fluid

By A. E. GARGETT,
Institute of Ocean Sciences, Patricia Bay, P.O. Box 6000, Sidney, B.C., V8L 4B2, Canada

T. R. OSBORN
U.S. Naval Postgraduate School, Monterey, CA 93940, U.S.A.

AND P. W. NASMYTH
Institute of Ocean Sciences, Patricia Bay

Gargett etal 1984

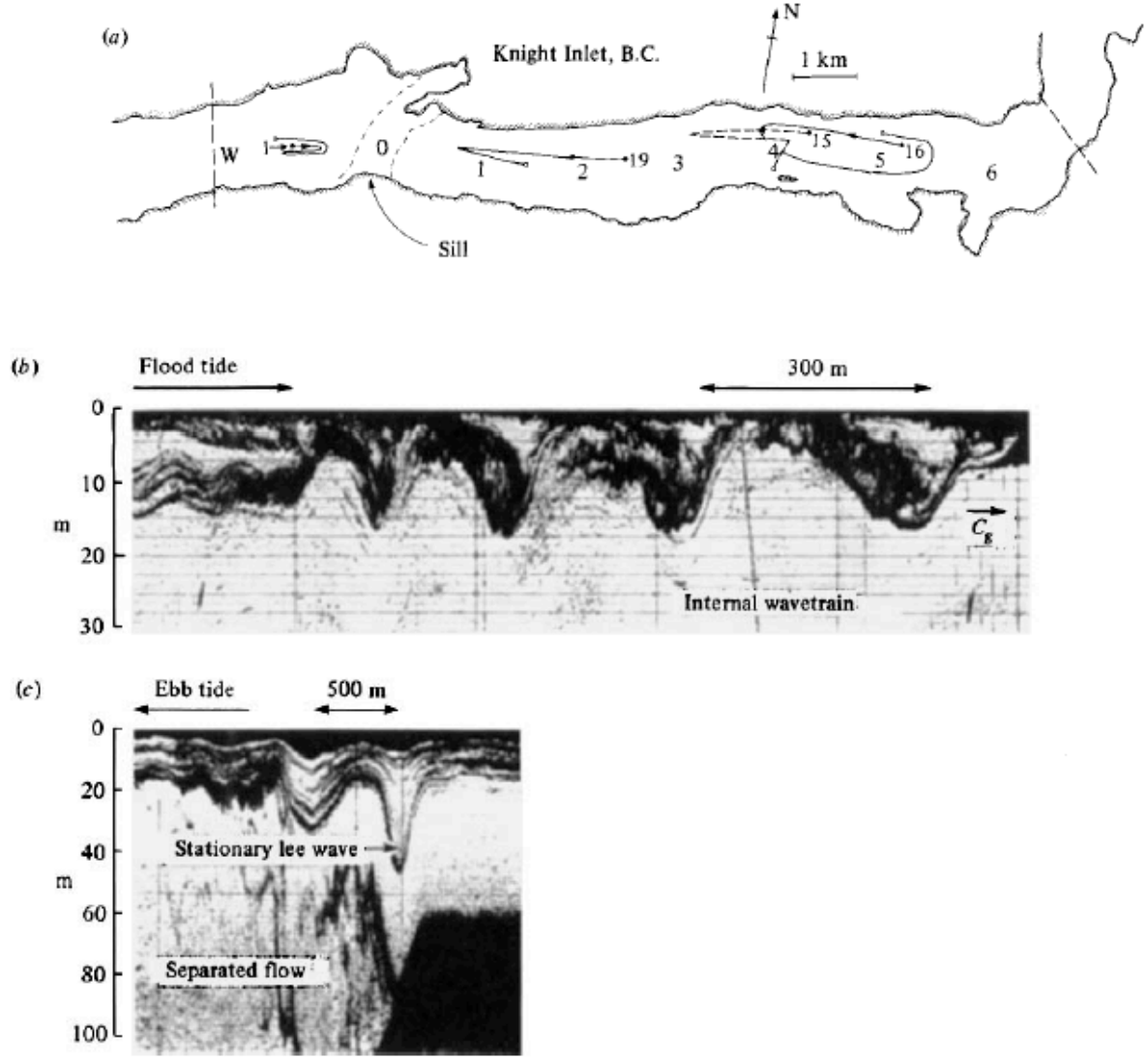

FIGURE 1. (*a*) Plan section of a portion of Knight Inlet, showing the location of the sill which divides the inlet into two basins. Turbulence measurements were taken from a submersible vehicle operating in the region between the dashed lines during the week of 15–22 November 1978. Submersible tracks shown (identified by date) supplied data used in this paper. Marked stations (W and 0–5) are locations of CTD profiles. (*b*, *c*) The two flow regimes in which measurements were taken are shown here (courtesy of David Farmer) in records from a 200 kHz echo-sounder operated during the week of turbulence measurements (horizontal scales are approximate): (*b*) measurements to the east of the sill were taken in an internal wave train released from the sill on the turn to flood tide; (*c*) To the west of the sill, measurements were taken in separated flow downstream of the sill on ebb tide.

Gargett etal 1984

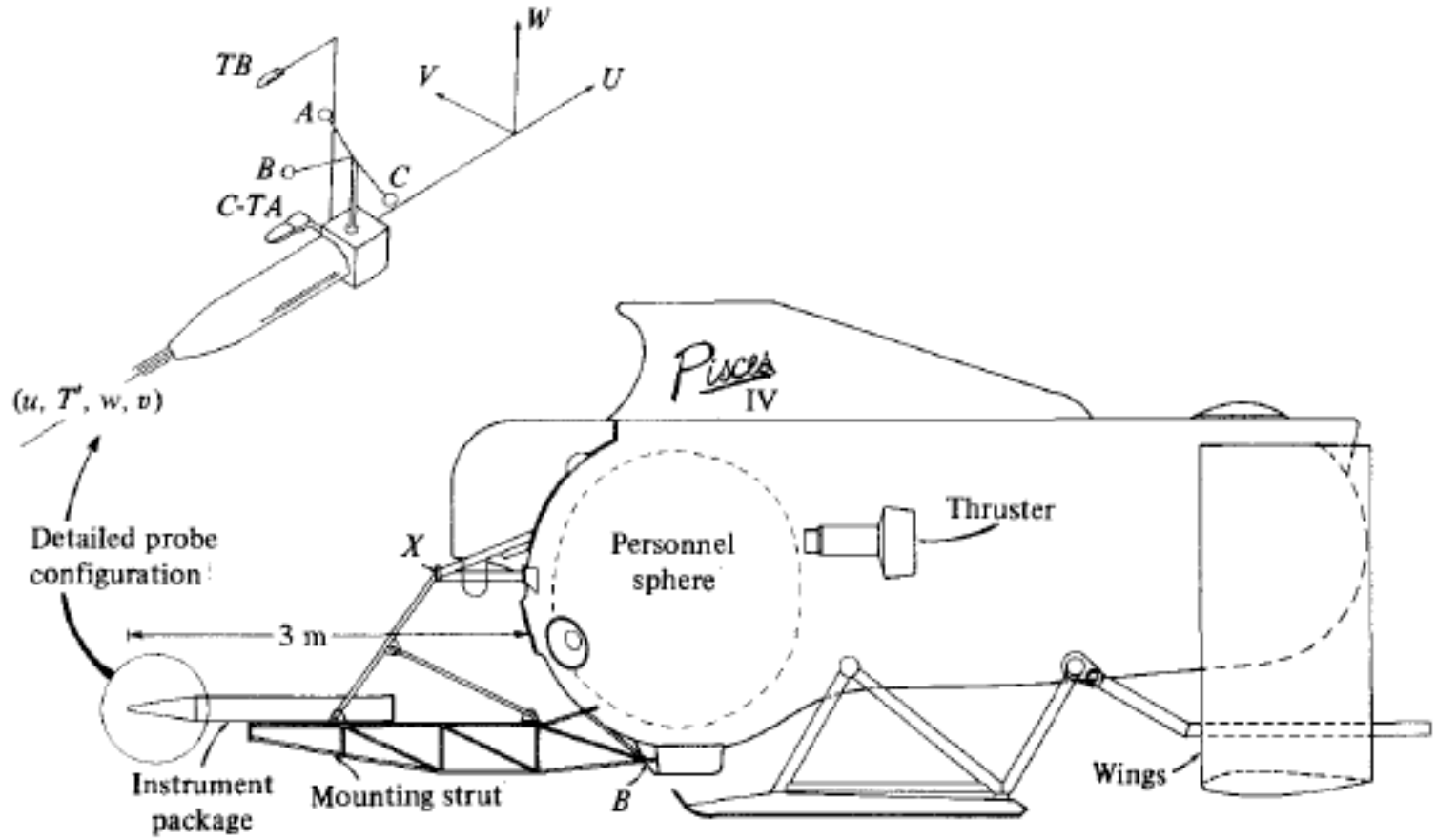

FIGURE 4. Schematic diagram of the submersible *Pisces IV* used to carry turbulence sensors. The inset shows the configuration of probes in a submersible-based coordinate system.

Gargett etal 1984

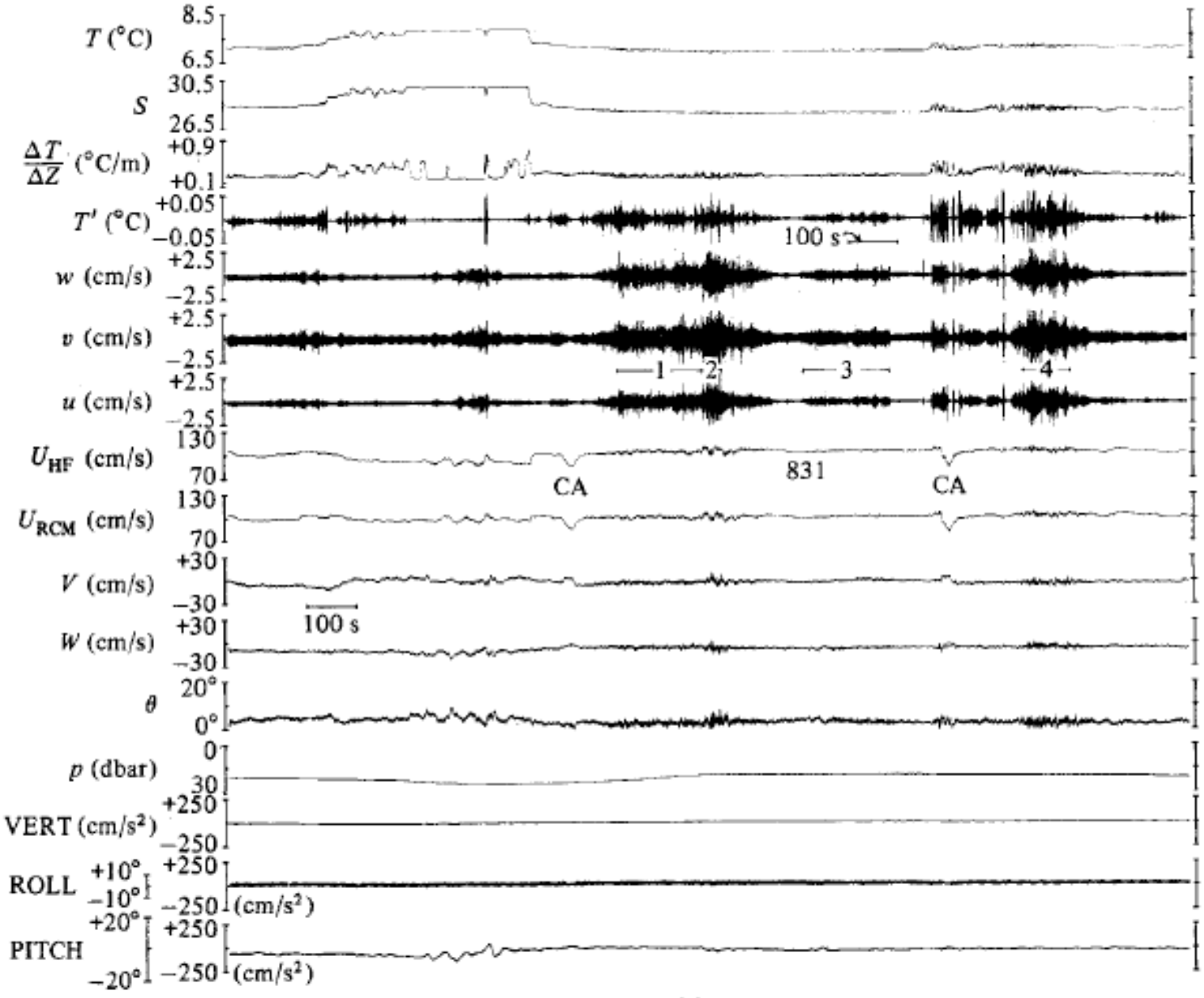

FIGURE 5. (*a*) Signals recorded as *Pisces IV* travelled within separated boundary flow west of the sill (W in figure 1). Signals are plotted as functions of time from left to right: because of *Pisces'* near-constant mean forward speed of ~ 1 m s^{-1}, they may as well be considered functions of distance, with 100 s $\approx$ 100 m. T and S are temperature and salinity measured at the level of the high-frequency sensors. $\Delta T/\Delta Z$ is an estimate of local vertical temperature gradient obtained by differencing the output of thermistors T_A and T_B (figure 4). T' is output from the cold-film temperature probe between 1 and 100 Hz, the same passband used for the vertical (w) and horizontal (v) cross-stream velocities measured by airfoil probes, and the horizontal streamwise velocity component (u) measured by the heated film. U_{HF} is a separate recorded version of the heated-film signal which contains velocity information to zero frequency. Immediately below it is U_{RCM}, an independent measure of forward speed calculated from a triplet of small ducted rotors located slightly behind and above the heated-film. V and W are horizontal and vertical cross-stream components of the flow as measured by these rotors, while θ is the instantaneous total angle of attack between the mean flow and the high-frequency sensors: an average value of $\theta \gtrsim 10°$ is sufficient for proper performance of both heated-film and airfoil sensors. Pressure p and three components of acceleration are measured by sensors at the same level but slightly behind the high-frequency sensors. The thickness of the accelerometer trace is due to submersible-produced vibrations.

Gargett etal 1984

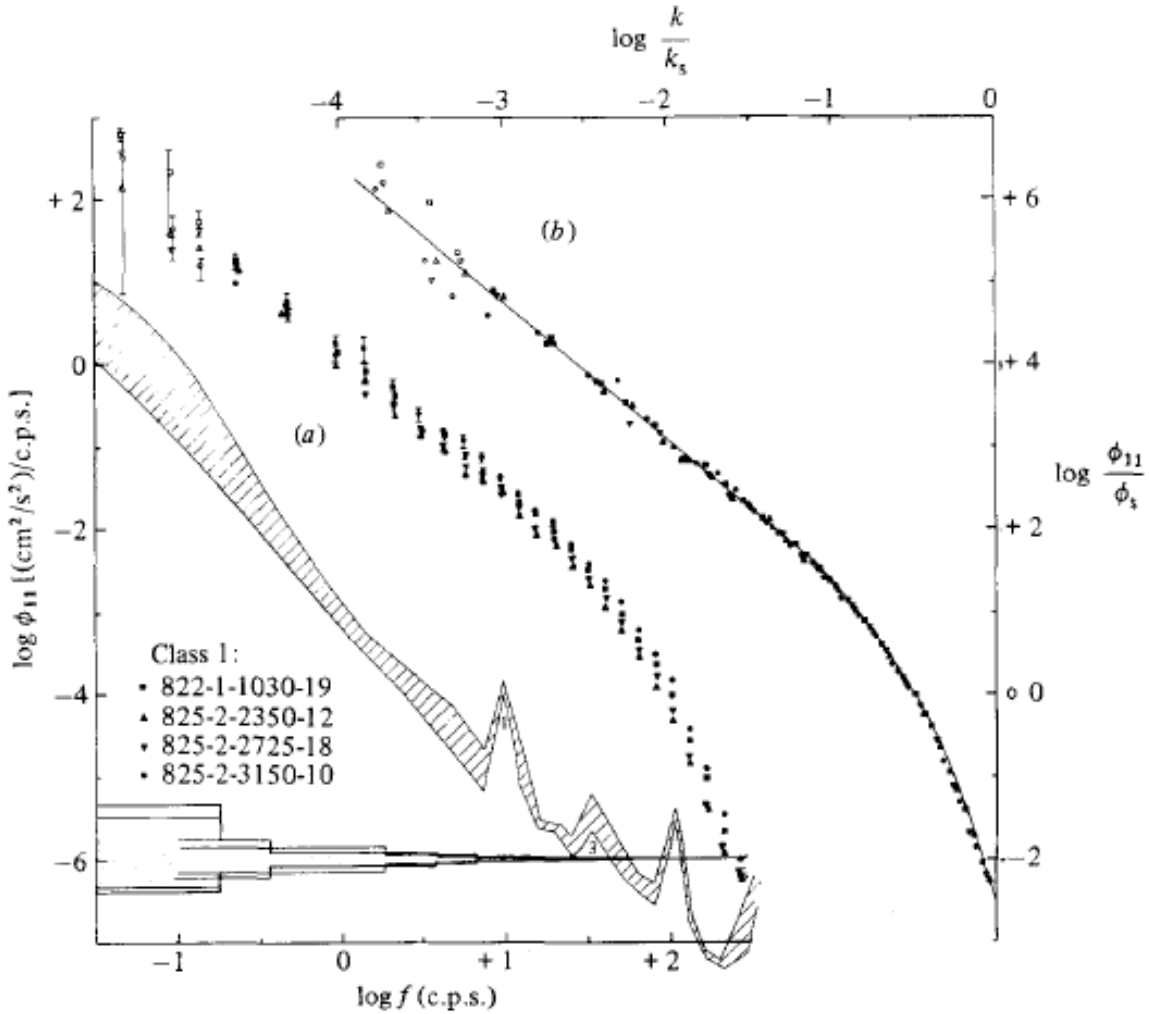

FIGURE 9. (*a*) Dimensional plots of ϕ_{11}, the u-component spectrum as a function of frequency for Class 1 records. Solid and open symbols denote respectively results from heated-film and rotor triplet measurements of u. Records are identified by Tape-File-Starting block-M, where M is the number of independent sample blocks averaged at the lowest wavenumber estimate of the solid symbols. Estimates of 95% confidence limits for records with the largest and smallest number of degrees of freedom are plotted at the bottom of this figure. Actual error bars calculated from variances of estimates at a single frequency are shown for these same two records. The two estimates are comparable, and both are smaller than plotted symbols at frequencies above $\sim$ 10 c.p.s. The shaded region is the observed range of noise spectra (figure 7). (*b*) The spectra of (*a*) converted to wavenumber space by the Taylor hypothesis, then non-dimensionalized by Kolmogoroff scales ϕ_s and k_s. The solid curve is a 'universal' curve derived from these data (§4).

Gargett etal 1984

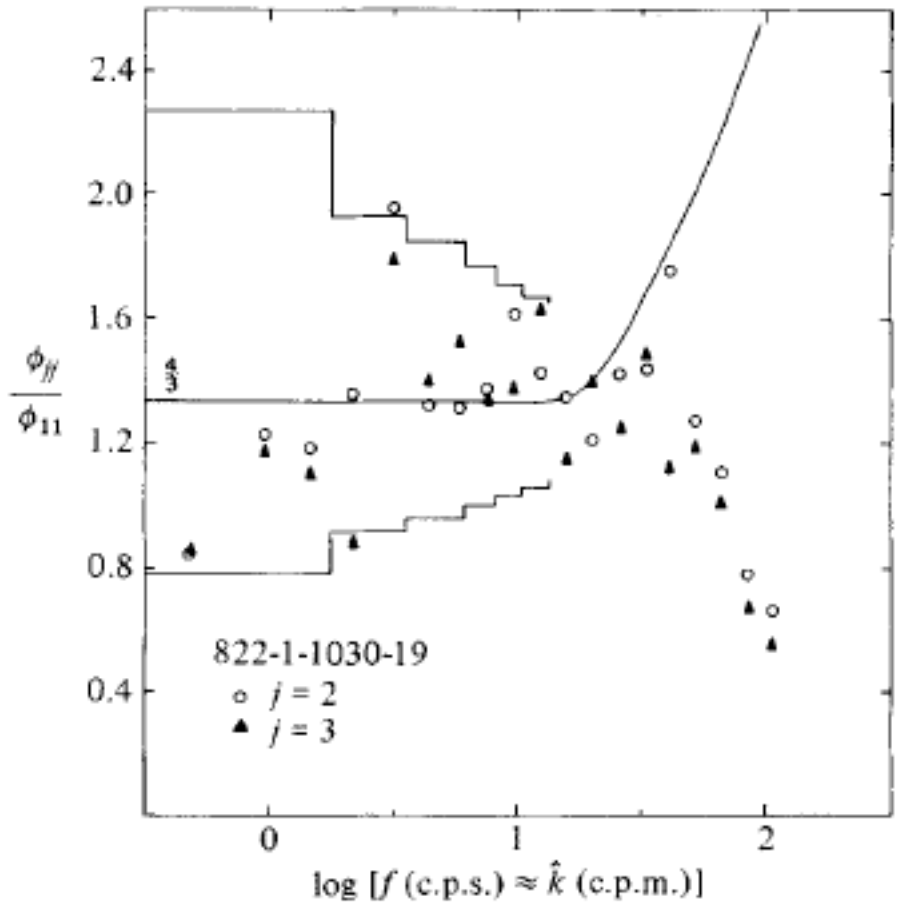

FIGURE 10. Ratios of cross-stream/streamwise velocity component spectra as a function of frequency (wavenumber) for record 822-1-1030-19. Measured values lie within statistical error bounds for over a decade in wavenumber, much stronger evidence of isotropy than the $-\frac{5}{3}$ slope of $\phi_{11}(k)$. The high-frequency (wavenumber) roll-off of the ratios, due to finite size of the airfoil probes, can be corrected by a response function determined from records, such as this, which exhibit evidence of isotropy before the scales affected by probe size (see Appendix). Subsequent presentations of cross-stream spectra include this response correction.

Gargett etal 1984

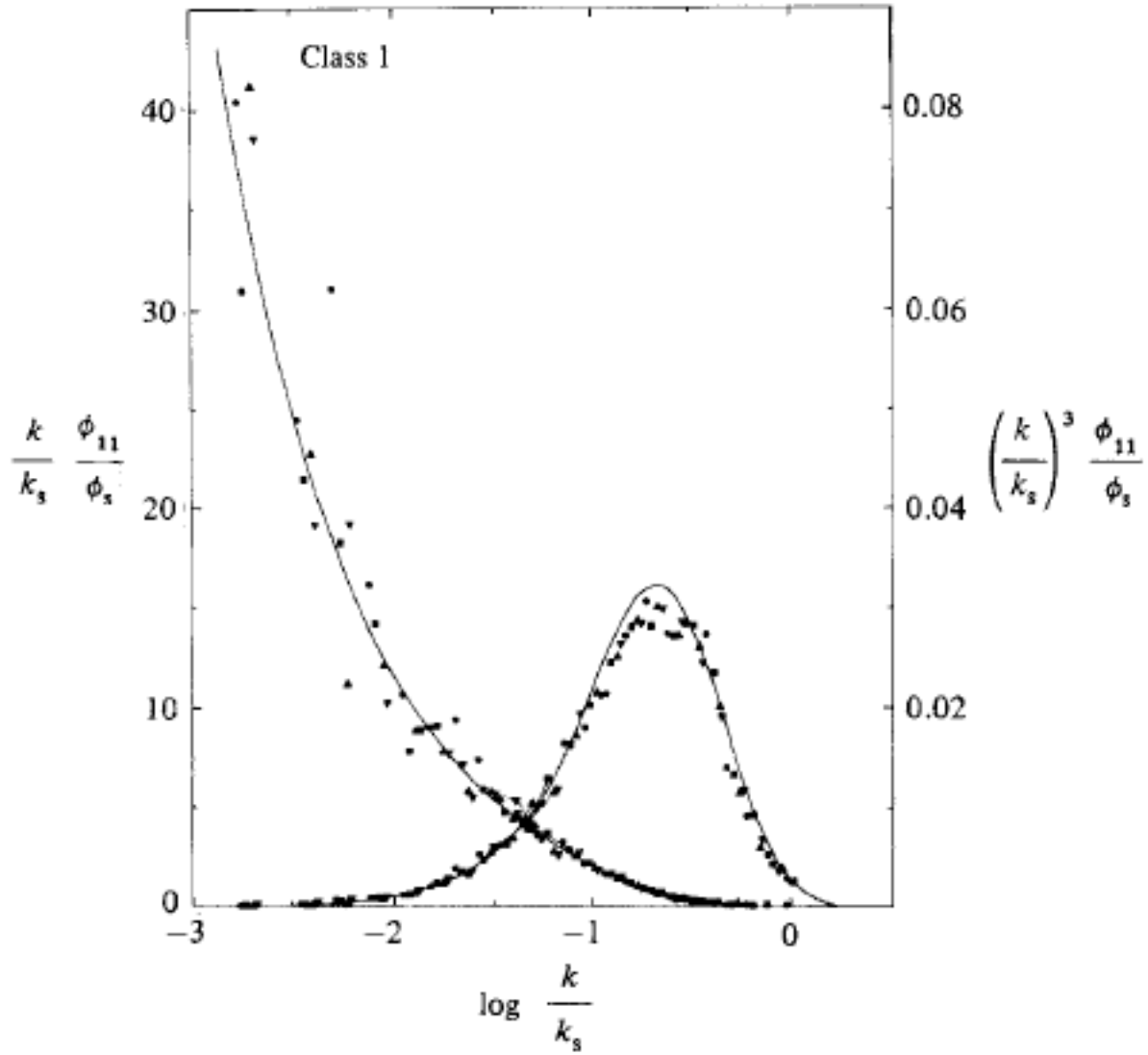

FIGURE 12. Variance-preserving energy and dissipation spectra for the stream-wise velocity spectra of figure 9. The estimate (14) of the kinetic-energy dissipation rate used in the Kolmogoroff variables,

$$\phi_s \equiv (\epsilon_1 \nu^5)^{\frac{1}{4}}\ \mathrm{cm^2\ s^{-2}/(rad\ m^{-1})} \quad \text{and} \quad k_s \equiv (\epsilon_1/\nu^3)^{\frac{1}{4}}\ \mathrm{rad\ m^{-1}},$$

is proportional to the area under this dissipation curve, which is completely resolved by the heated-film measurement.

Gargett etal 1984

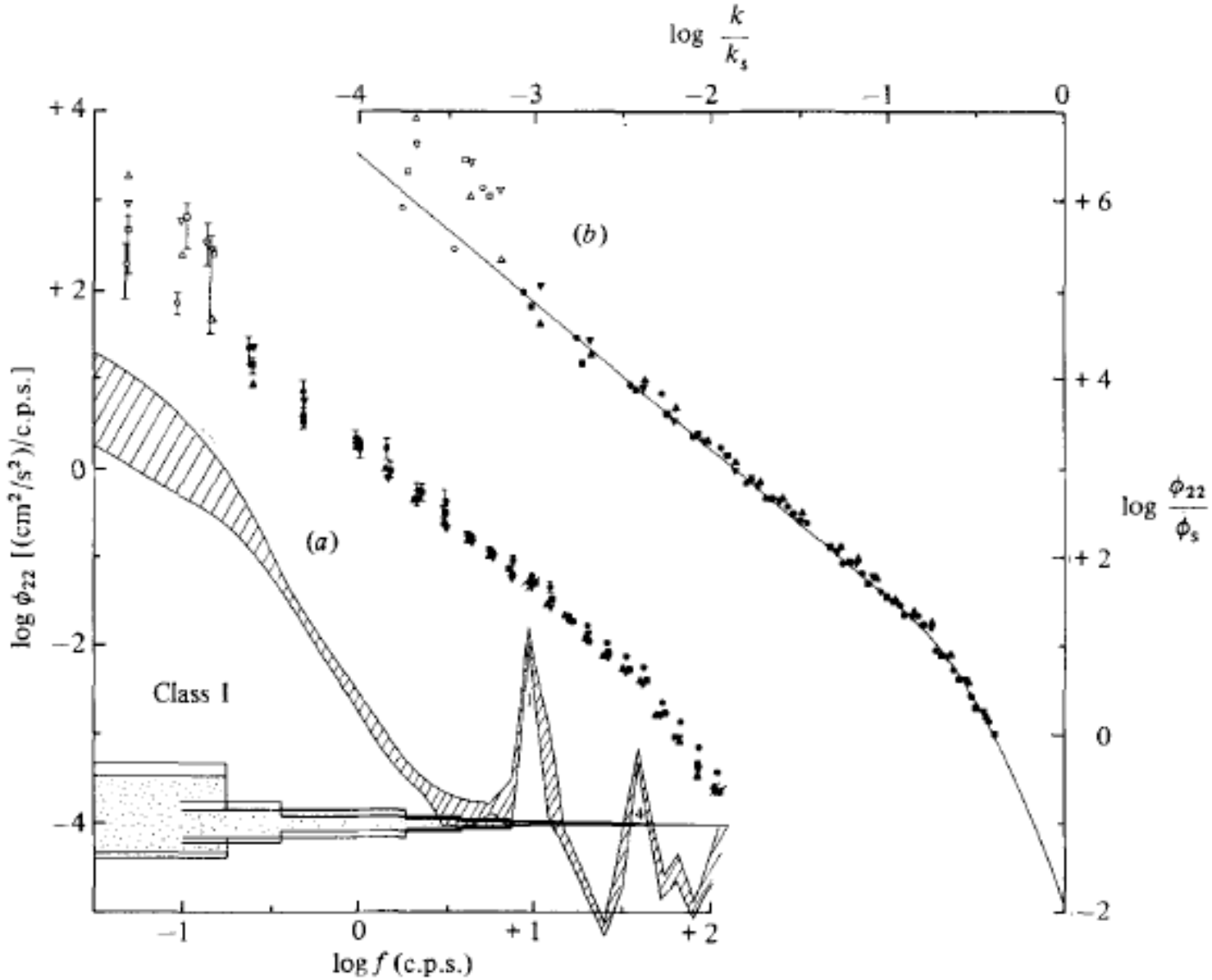

FIGURE 13. (*a*) Dimensional plots of ϕ_{22}, the v-component cross-stream spectrum as a function of frequency for Class 1 records. Solid and open symbols denote respectively results from airfoil probe and rotor triplet measurements of v. Flagged points (less than 3 times the upper noise level spectrum) are removed from further analysis. (*b*) Spectra non-dimensionalized by Kolmogoroff scales ϕ_s and k_s.

Gargett etal 1984

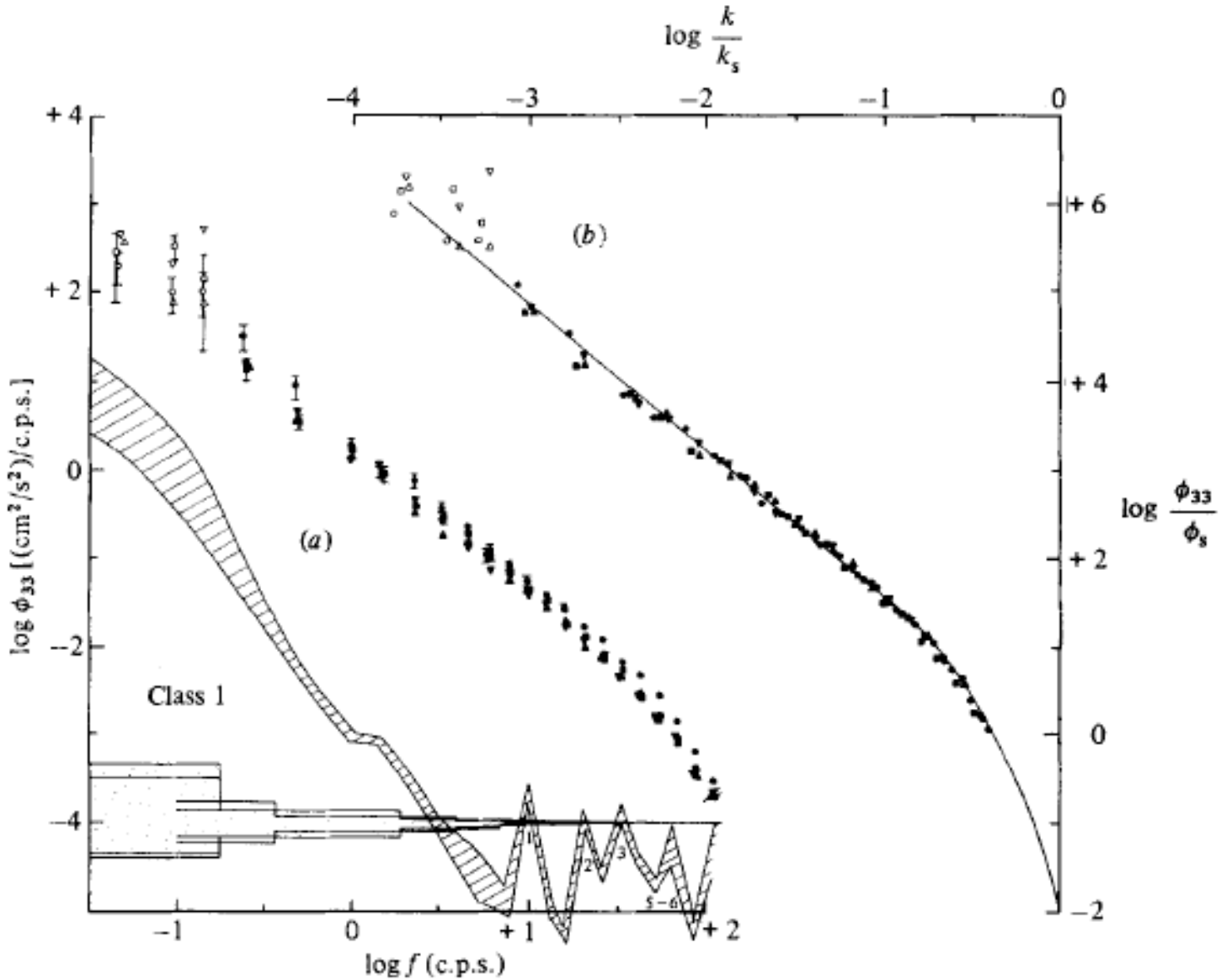

FIGURE 14. (*a*) Dimensional plots of ϕ_{33}, the w-component cross-stream spectrum as a function of frequency for Class 1 records. Solid and open symbols denote respectively results from airfoil probe and rotor-triplet measurements of w. Flagged points (less than 3 times the upper noise level spectrum) are removed from further analysis. (*b*) Spectra non-dimensionalized by Kolmogoroff scales ϕ_s and k_s.

Gargett etal 1984

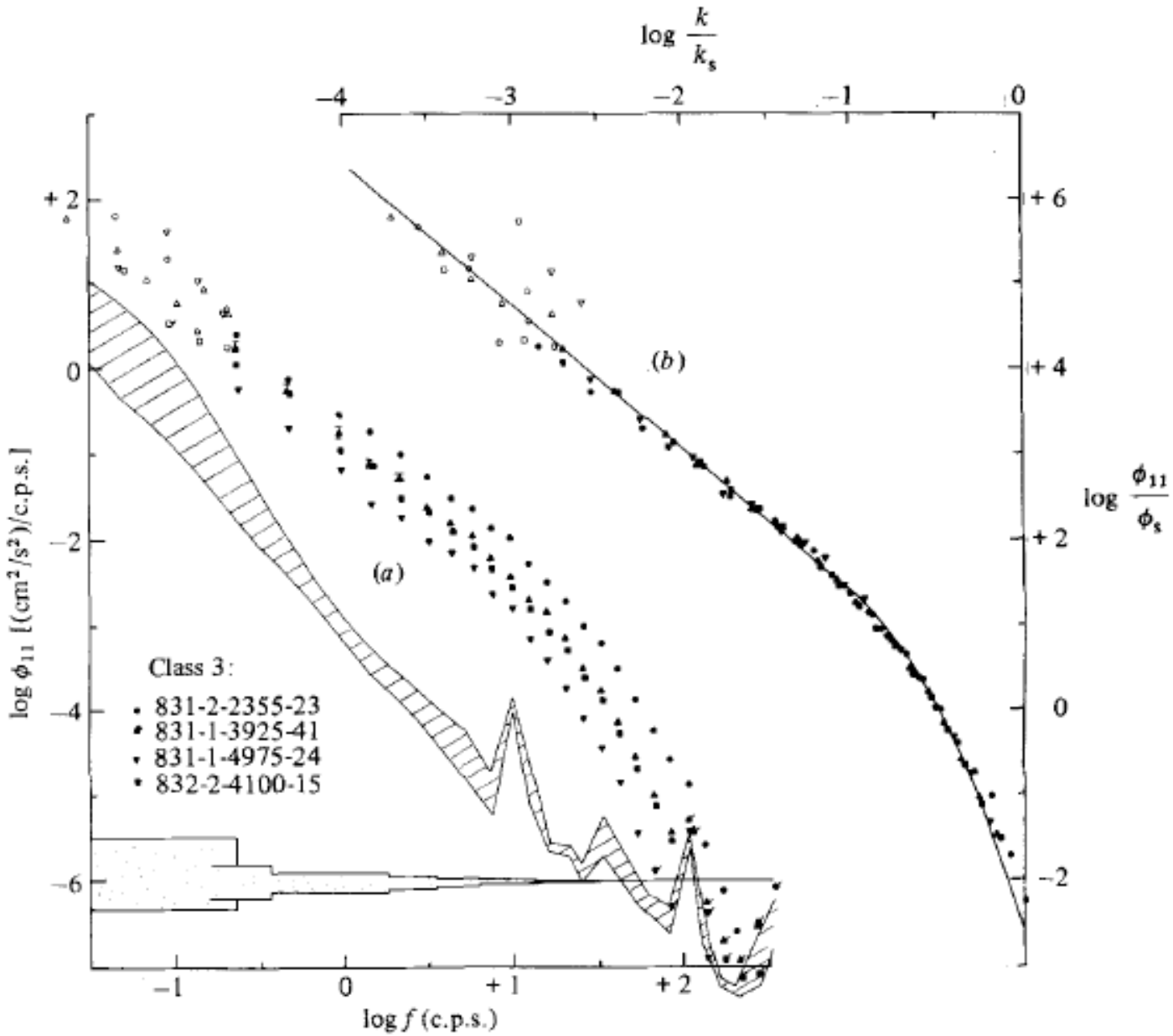

FIGURE 21. (*a*) Dimensional plots of ϕ_{11} as a function of frequency for Class 3 records: for further details see caption to figure 17(*a*). (*b*) Kolmogoroff-scaled spectra: the slight tendency for ϕ_{11} to fall below the universal curve in the inertial subrange is not statistically significant here, but will become so in the next class.

Gargett etal 1984

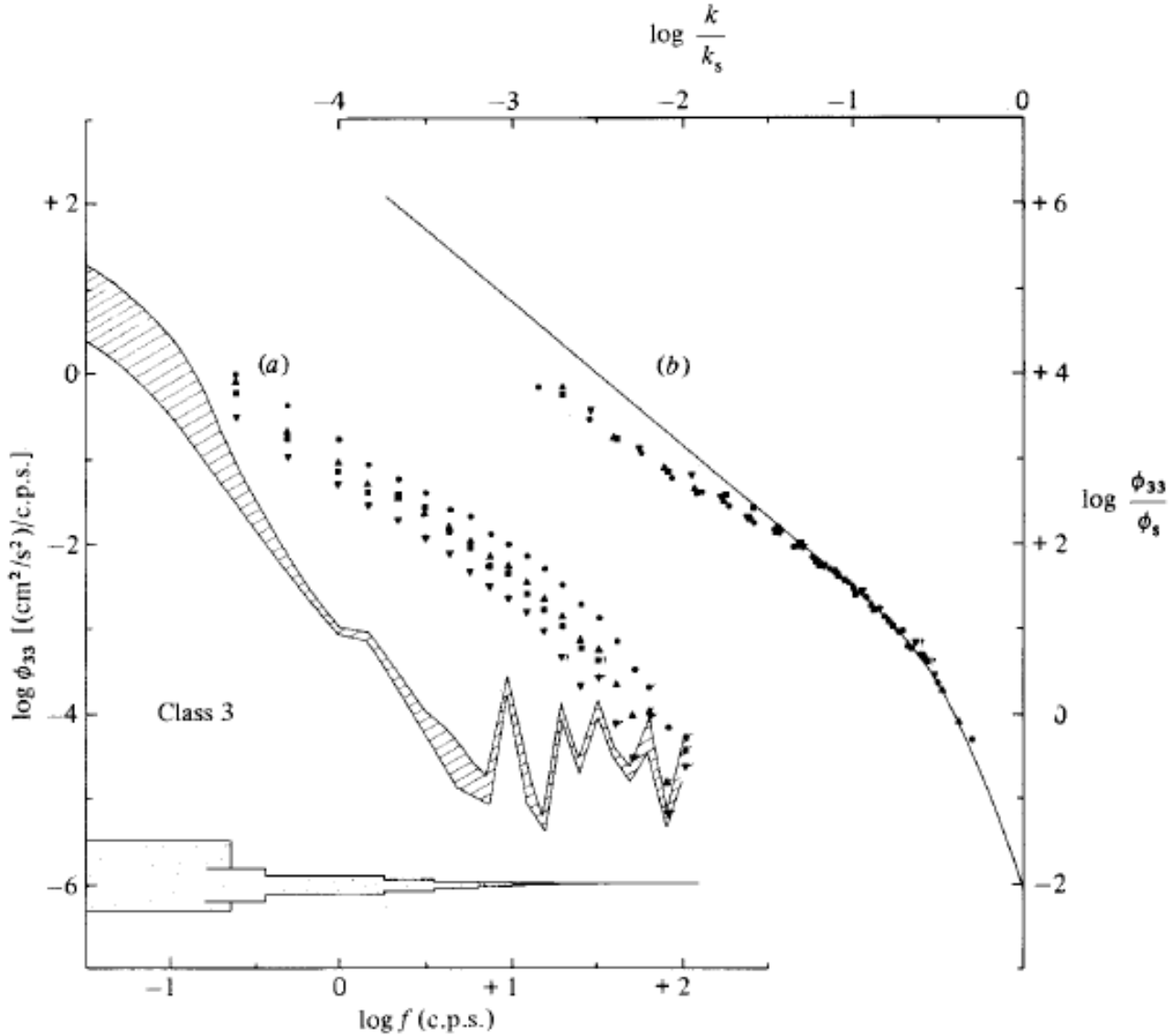

FIGURE 22. (*a*) Dimensional plots of ϕ_{33} as a function of frequency for Class 3 records. Low-frequency estimates from the rotor triplet are almost all at noise level and have been omitted: solid symbols are results from the *w*-component airfoil. Lower signal levels lead to increased rejection of high-frequency estimates; second and third harmonics of the fundamental vibration frequency are also starting to cause rejection or possible contamination (?) of the lower energy records. (*b*) Kolmogoroff-scaled spectra: the ϕ_{22} spectra (not shown) are statistically identical.

Gargett etal 1984

class 4

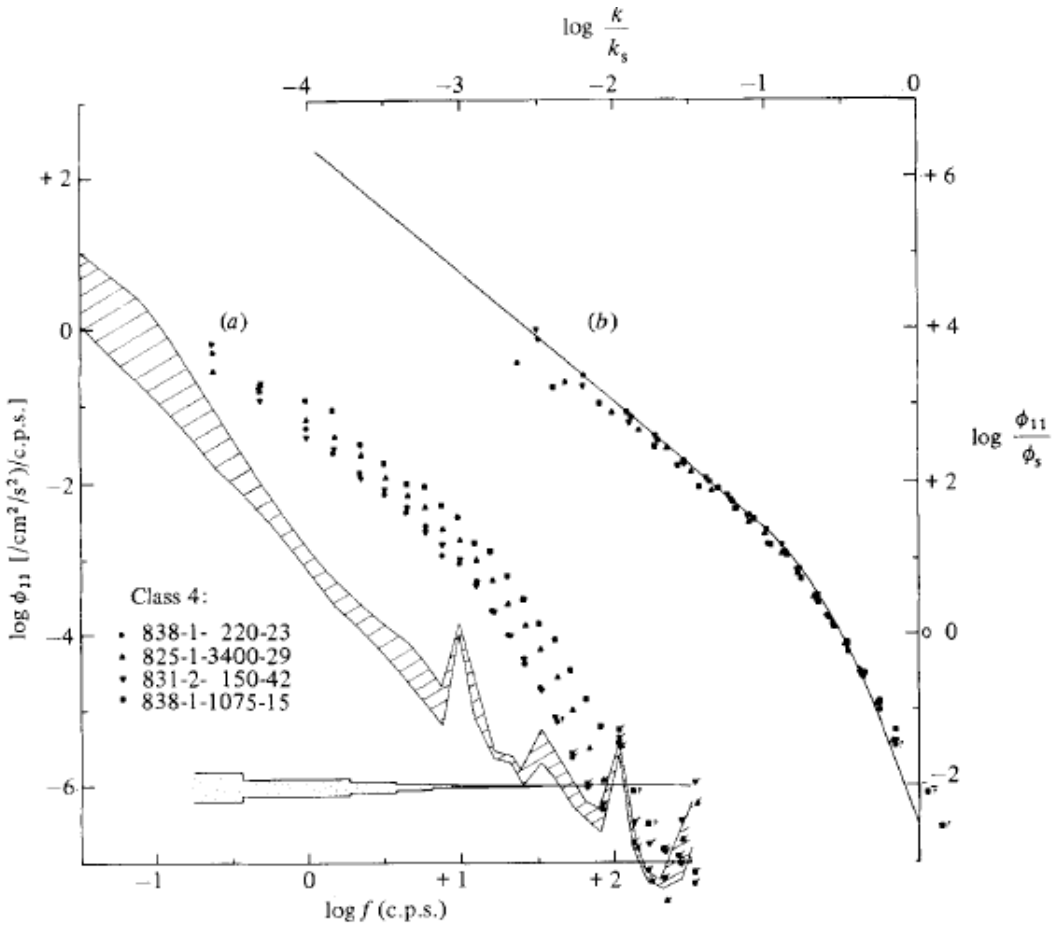

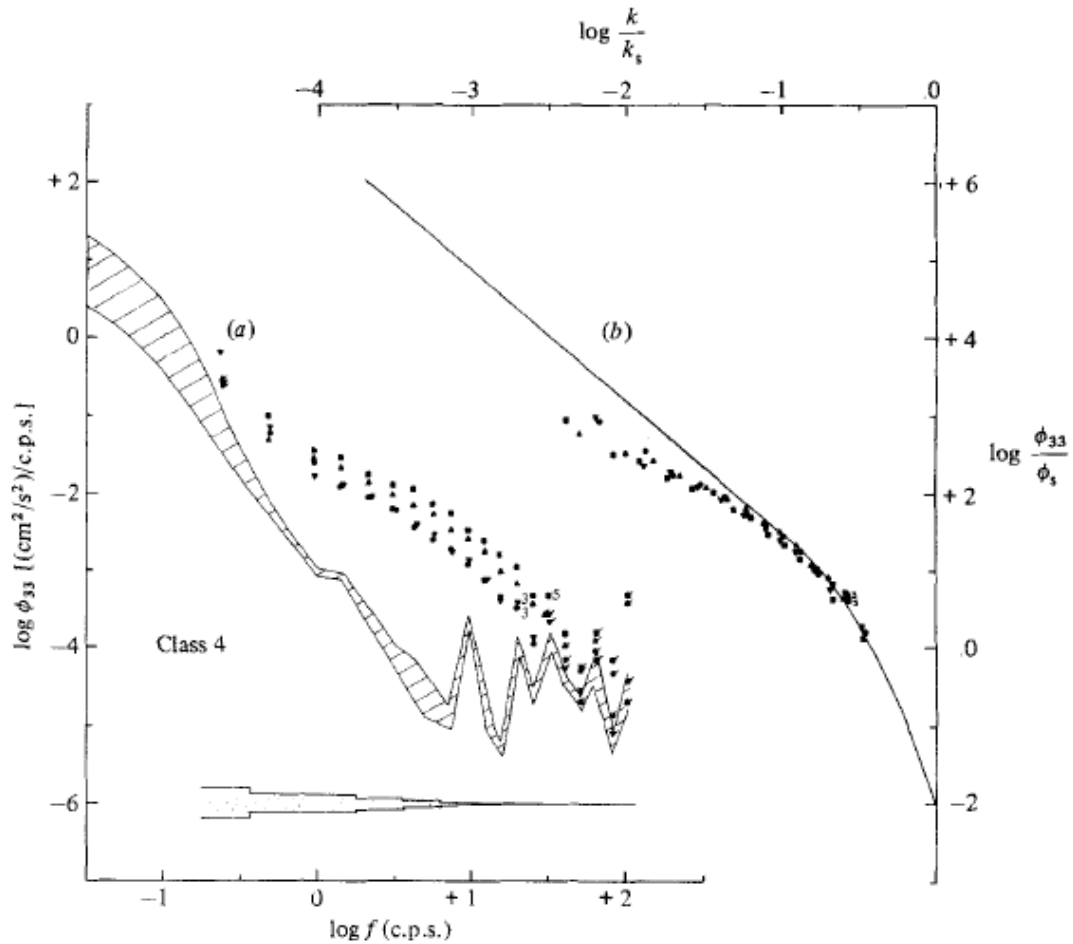

Gargett etal 1984

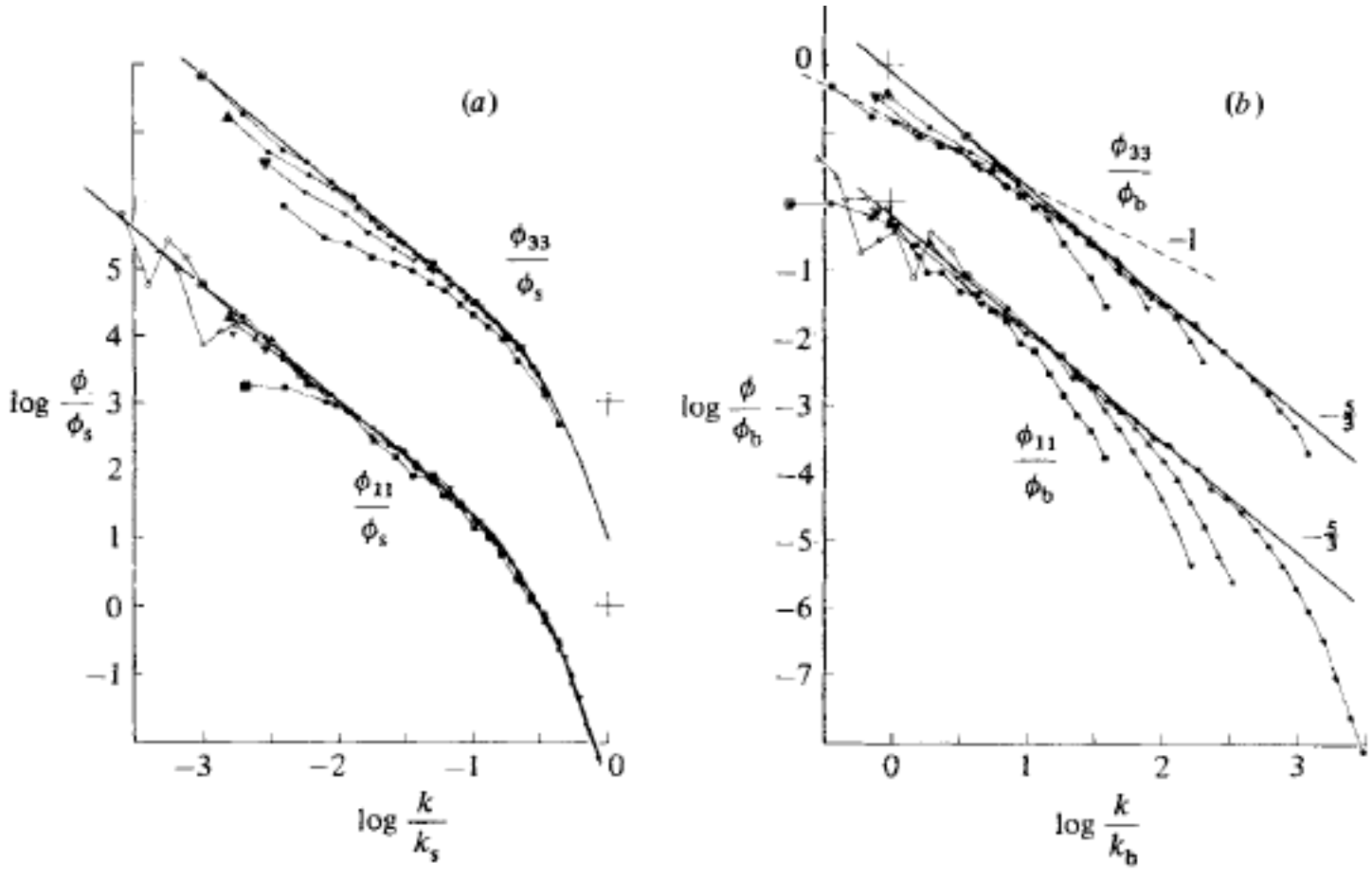

Gargett etal 1984

Gargett etal 1984

Gargett etal 1984

Gargett etal 1984

Gargett etal 1984